



# Facts and Fictions About [<sup>18</sup>F]FDG versus Other Tracers in Managing Patients with Brain Tumors

## It Is Time to Rectify the Ongoing Misconceptions

Nadia Withofs, MD, PhD<sup>a,b,\*</sup>, Rakesh Kumar, MBBS, DRM, DNB, MNAMS, PhD<sup>c</sup>, Abass Alavi, MD<sup>d</sup>, Roland Hustinx, MD, PhD<sup>a,b</sup>

### KEYWORDS

- Brain tumor • Neuro-oncology • FDG • FDOPA • FET • PET

### KEY POINTS

- [<sup>18</sup>F]FDG positron emission tomography/computed tomography scanning is a valuable tool for characterizing suspicious MRI lesions, and identifying recurrence/persistence of high-grade gliomas.
- [<sup>18</sup>F]FET better defines gliomas boundaries within the normal brain than with [<sup>18</sup>F]FDG, including low-grade gliomas, although it can be falsely negative in up to 30% of World Health Organization grade 2 gliomas.
- The specificity of amino acids positron emission tomography is not perfect. False-positive results occur in a wide variety of nontumor pathologic conditions.
- Both [<sup>18</sup>F]FDG and radiolabeled amino acids positron emission tomography performances should be further assessed, integrating gliomas molecular profile presented in the latest World Health Organization CNS5 classification.

### INTRODUCTION

Brain metastases are the most common malignant brain tumor in adults, most frequently related to lung cancer, breast cancer, and melanoma.<sup>1</sup> Brain metastases incidence is distinctly higher than that of primary malignant brain tumors. Overall, the latter account for less than 1% of all invasive cancer cases in the United States, but they are the second

most common cancer in children and adolescents and the leading cause of cancer death among males aged less than 40 years and females aged less than 20 years.<sup>2</sup> The fifth edition of the World Health Organization (WHO) classification of tumors of the central nervous system (WHO CNS5) published in 2021 increasingly incorporates molecular diagnostic markers to histology and immunohistochemistry.<sup>3</sup> Such evolution complexifies the

<sup>a</sup> Division of Nuclear Medicine and Oncological Imaging, Department of Medical Physics, CHU of Liege, Quartier Hopital, Avenue de l'Hopital, 1, Liege 1 4000, Belgium; <sup>b</sup> GIGA-CRC in vivo imaging, University of Liege, GIGA CHU - B34 Quartier Hôpital Avenue de l'Hôpital, 11, 4000 Liège, Belgium; <sup>c</sup> Diagnostic Nuclear Medicine Division, All India Institute of Medical Sciences, New Delhi 110029, India; <sup>d</sup> Department of Radiology, Hospital of the University of Pennsylvania, 3400 Spruce Street, Philadelphia, PA 19104, USA

\* Corresponding author: Division of Nuclear Medicine and Oncological Imaging, Department of Medical Physics, CHU of Liege, Quartier Hopital, Avenue de l'Hopital, 1, Liege 1 4000, Belgium.

E-mail address: nwwithofs@chuliege.be

distinction between low-grade and high-grade gliomas. For example, the presence of 1p/19q codeletion and *IDH* mutation in patients with WHO grade 2 diffuse gliomas is associated with a more favorable outcome. By contrast, patients with *IDH*-mutant astrocytoma and a *CDKN2A/B* homozygous deletion are doomed with a poor prognosis, regardless of the WHO glioma grade.<sup>4,5</sup> In the present review, we avoided using the terms low-grade and high-grade gliomas and replaced these terms by WHO grade 2 (and 1) versus WHO grade 3 and 4 gliomas, respectively, unless otherwise stated.

MRI is the first-choice imaging technique for brain tumors.<sup>5–8</sup> The T2-weighted and/or T2 fluid-attenuated inversion recovery is performed for tumor detection and delineation, but cannot reliably differentiate tumor from other conditions, such as demyelination, ischemic injury, and edema, especially once treatment, for example, radiation therapy and/or chemotherapy, has been initiated.<sup>9</sup> Moreover, inflammation induced by immunotherapies can alter T2 signal intensity.<sup>6</sup> Diffusion-weighted imaging sequence and apparent diffusion coefficient (ADC) measurements are used to characterize brain lesions and assess tumor response to treatments but similarly high ADC values can be observed in high-grade gliomas as well as in necrotic areas and abscesses.<sup>9–11</sup> Thin-section 3D T1-weighted sequences before and after injection of a gadolinium-based contrast agent identifies brain areas with blood-brain barrier (BBB) disruption. The latter is usually present in WHO grade 3 and 4 gliomas but also in WHO grade 2 oligodendroglomas, lymphomas, and other non-neoplastic conditions.<sup>6,12</sup> Treatments, including radiation therapy, antiangiogenic therapies and immunotherapies can induce transient changes in contrast enhancement that can be misleading in assessing response to treatment.<sup>6</sup> The MR spectroscopy can contribute to lesion characterization, including distinction of tumor from non-neoplastic conditions, for example, post-therapy changes, but it lacks both sensitivity and specificity.<sup>13</sup> Perfusion MRI, dynamic contrast enhanced and dynamic susceptibility contrast MRI, allows distinction between WHO grade 3 and 4 gliomas and WHO grade 2 gliomas at diagnosis using relative cerebral blood volume (rCBV) values measured using dynamic susceptibility contrast MRI with high sensitivity (95%), but low specificity (57%), mainly due to WHO grade 2 oligodendroglomas with elevated rCBV.<sup>12–14</sup> At diagnosis, perfusion MRI can guide biopsy to areas of higher WHO grade tumor. Within 24 to 48 hours after surgery, the extent of resection can be assessed by MRI. Advanced MRI techniques (eg, diffusion-weighted imaging

and ADC values; dynamic susceptibility contrast/dynamic contrast enhanced MRI and rCBV values; and MR spectroscopy) showed high diagnostic accuracy in the differentiation between treatment-induced changes (eg, pseudoprogression and radiation necrosis) and true progression, with both sensitivity and specificity of more than 85%.<sup>6,15–17</sup>

Even when multiple MRI sequences are performed, MRI still has limitations.<sup>8,18</sup> Positron emission tomography (PET) combined with computed tomography (CT) scan (or MRI) is not recommended routinely but contributes to the management of brain tumors from diagnosis to follow-up, in particular when recurrence is suspected.<sup>19–21</sup> Brain tumor cells metabolic adaptation is driven by tumor's phenotype (eg, mutation of the gene *IDH1* coding for isocitrate dehydrogenase 1, component involved in the tricarboxylic acid cycle) and microenvironment changes (eg, frequent hypoxic environment).<sup>22</sup> The brain is a special environment restricted by the BBB; gliomas and cancer cells take up nutrients from the extracellular environment, including glucose, acetate, glutamine and other amino acids (AAs) and fatty acids, to ensure tumor growth.<sup>22</sup>

Borja and colleagues<sup>23</sup> recently presented the use of PET tracers for brain tumor imaging for tumor grading, delineation, and treatment response assessment. The present work aims at further discussing the role of 2-[<sup>18</sup>F]fluoro-2-deoxy-D-glucose ([<sup>18</sup>F]FDG) and alternative PET tracers in the management of brain tumors.

## 2-[<sup>18</sup>F]FLUORO-2-DEOXY-D-GLUCOSE

2-[<sup>18</sup>F]fluoro-2-deoxy-D-glucose (<sup>[18]</sup>F]FDG) is transported across the intact BBB by glucose transporters (GLUT), mainly GLUT1 and GLUT3, and [<sup>18</sup>F]FDG accumulation in brain tumors does not depend on BBB disruption.<sup>24,25</sup> Glucose is a major energy substrate of cancer cells in brain, even in the presence of oxygen (aerobic glycolysis; Warburg effect). GLUT1 and GLUT3 are upregulated in tumors, especially in aggressive tumors, and GLUT3 upregulation has been correlated with poor survival.<sup>24,26</sup> The glucose metabolic rate correlates with both GLUT expression and the cell proliferation rate.<sup>26</sup> Various methods have been used to quantify glucose metabolic rate of brain lesions using [<sup>18</sup>F]FDG PET/CT scans, but none of them have been validated and there is no role for such measurements in routine clinical practice.<sup>27</sup> As a rule of thumb, the WHO grade 3 and 4 gliomas are more likely to show high [<sup>18</sup>F]FDG uptake, higher or similar to gray matter, whereas [<sup>18</sup>F]FDG uptake of WHO grade 2 glioma tends to be similar

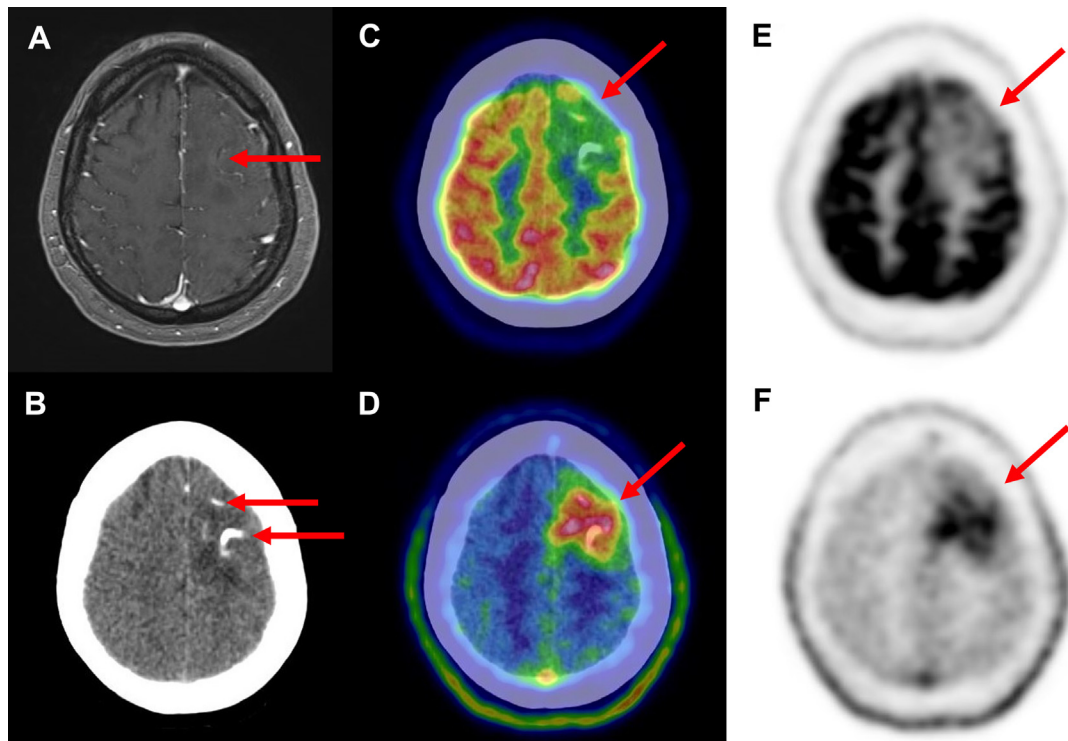


**Fig. 1.** Brain images of a 39-year-old patient with a left frontal lesion with mild enhancement after gadolinium injection in MR images (*A*, postgadolinium T1-weighted MRI; red arrow) and increased perfusion described by multiparametric MRI (not shown). The CT images of the PET/CT scans showed calcifications (*B*, CT scan of PET/CT scan; red arrows), characteristic of oligodendriogliomas. The lesion seemed to be hypometabolic in [<sup>18</sup>F]FDG PET images (*C*, fused PET/CT scan; *E*, PET image, SUV scale of 0–8; red arrows) with [<sup>18</sup>F]FDG uptake (maximum SUV 5.6) slightly higher than white matter and lower than gray matter. The [<sup>18</sup>F]FDG TBR<sub>max</sub> (maximum tumoral SUV/maximum SUV in the contralateral healthy hemisphere) estimated at 0.5 suggested a WHO grade 2 glioma.<sup>29</sup> The [<sup>18</sup>F]FET PET images (*D*, fused PET/CT scan; *F*, PET image, SUV scale 0–5; red arrows) allowed to better estimate the extent of the lesion; the [<sup>18</sup>F]FET TBR<sub>max</sub> (maximum tumoral SUV/mean SUV in the contralateral healthy hemisphere), estimated at 4.5, suggested a WHO grade 3 andand 4 glioma.<sup>75</sup> The pathologic diagnosis was an oligodendrolioma WHO grade 2, IDH-mutant (IDH1 p.R132 mutation), and 1p/19q-codeleted. The [<sup>18</sup>F]FDG TBR<sub>max</sub> correctly predicted the WHO grade 2 glioma whereas [<sup>18</sup>F]FET TBR<sub>max</sub> overestimated it.

to white matter. As a result, they are most of the time not seen, or present as cortical hypometabolic areas. One method helpful to differentiate those lesions is to calculate the tumor to contralateral normal brain standardized uptake value (SUV) ratios (TBRs). TBR cutoff values help to differentiate WHO grade 3 and 4 from WHO grade 1 to 2 gliomas (eg, a TBR cutoff value of 0.6 for tumor-to-cortex maximum SUV ratio is often used).<sup>27–29</sup> Although the [<sup>18</sup>F]FDG TBR is usually higher in WHO grade 3 andand 4 gliomas, it could also be similarly increased in WHO grade 1 pilocytic astrocytoma and WHO grade 2 gliomas with oligodendroglial component, which somehow limits the accuracy of [<sup>18</sup>F]FDG PET/CT scans to predict glioma grade at diagnosis (Fig. 1).<sup>30,31</sup> Moreover, in the differential diagnosis between neoplastic and non-

neoplastic lesions, [<sup>18</sup>F]FDG PET/CT scans can be falsely negative in WHO grade 2 gliomas or metastases, and it can be falsely positive in inflammatory brain lesions.<sup>19,32,33</sup> Nonetheless, the combination of metabolic and MRI features is usually quite efficient for characterizing those lesions. Furthermore, [<sup>18</sup>F]FDG uptake is an independent prognostic marker in primary central nervous system lymphoma and in WHO grade 4 gliomas at diagnosis and after treatment initiation.<sup>28,34–36</sup> Environmental conditions influence [<sup>18</sup>F]FDG transport at the BBB and in brain tumors, for example, hyperglycemia associated with diabetes or hypoxia.<sup>24</sup> The major drawback of [<sup>18</sup>F]FDG is the uptake in brain cells, including astrocytes, microglia and neurons, and hampering precise tumor delineation.<sup>24</sup>

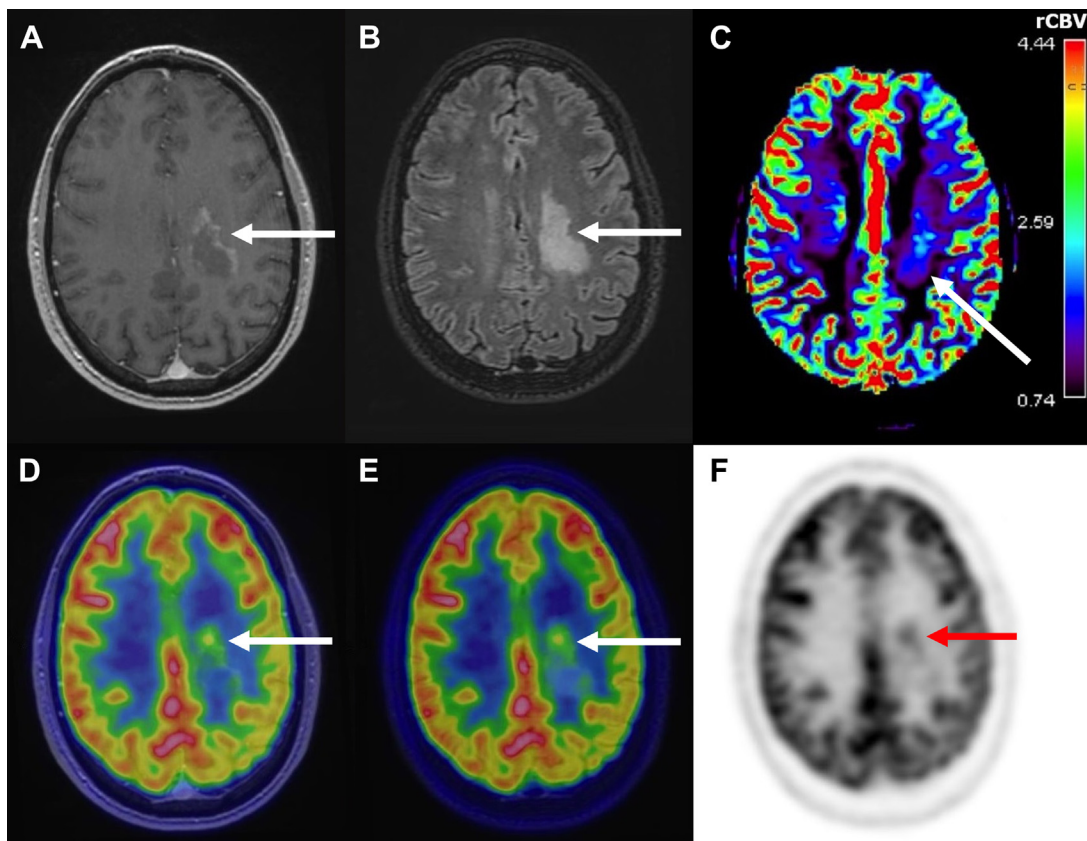


**Fig. 2.**  $[^{18}\text{F}]$ FDG PET and MR images of a 34-year-old patient who presented with neurologic deficits related to a left frontoparietal brain lesion. The postgadolinium T1-weighted MR images demonstrated peripheral contrast enhancement (A, white arrow), whereas the T2/fluid-attenuated inversion recovery (FLAIR) sequence allowed visualization of the lesion with better contrast (B, white arrow). The perfusion MR images showed increased rCBV (C, white arrow). The  $[^{18}\text{F}]$ FDG PET images highlighted a tumor area with high  $[^{18}\text{F}]$ FDG uptake in the most anterior part of the lesion (D, E, fused PET/MRI, white arrows; F, PET image, SUV scale 0–10; lesion maximum SUV, 6.1; TBR<sub>max</sub>, 0.6; red arrow), which therefore was suggested as the best biopsy site to neurosurgeon. The pathologic diagnosis was a WHO grade 4 glioma.

Even though  $[^{18}\text{F}]$ FDG PET/CT alone has limited accuracy in the diagnosis of a suspected brain tumor, it can be a reliable imaging technique to guide stereotactic brain biopsy to tumor areas with the highest  $[^{18}\text{F}]$ FDG uptake, more likely to correspond with WHO grade 3 and 4 gliomas, avoiding sampling errors and undergrading gliomas based on MRI only (Fig. 2).<sup>37–39</sup> Pirotte and colleagues,<sup>37,40</sup> in a work published in 2004 when more advanced MRI techniques such as perfusion were in its infancy, were able to use  $[^{18}\text{F}]$ FDG PET for guiding stereotactic biopsy in almost one-half of patients ( $n = 14/32$ ). The combination of  $[^{18}\text{F}]$ FDG PET and multiparametric MRI might significantly increase the performance of  $[^{18}\text{F}]$ FDG PET for stereotactic biopsy target definition but this has not been addressed in the era of multiparametric MRI.<sup>13</sup> Note that in case of suspected primary central nervous system lymphoma,

additional whole-body  $[^{18}\text{F}]$ FDG PET/CT scanning is recommended for staging.<sup>41</sup>

$[^{18}\text{F}]$ FDG PET/CT scanning can be considered in combination with multiparametric MRI for WHO grade 3 and 4 gliomas or  $[^{18}\text{F}]$ FDG-avid metastases for differentiating tumor recurrence from treatment-induced changes induced by BBB breakdown and edema, including pseudoprogression and radiation necrosis.<sup>7,19,27,36,42</sup> In the follow-up MRI, the extent of contrast enhancement in T1-weighted sequence or T2/fluid-attenuated inversion recovery-weighted MR signal can temporarily increase within the first 3 months after radiation therapy completion in up to two-third of patients with WHO grade 4 gliomas, mimicking progression. And, there is an increased likelihood of pseudoprogression in WHO grade 4 gliomas with O<sup>6</sup>-methylguanine-DNA methyltransferase (MGMT) promoter methylation.<sup>7,36,43</sup>

Beyond 6 months and up to several years after radiation therapy for metastases or gliomas, radiation necrosis can occur within the irradiated field in up to one-quarter of cases, with the risk increasing with total radiation dose, irradiated volume, and additional chemotherapy.<sup>7,36</sup> [<sup>18</sup>F]FDG PET/CT scanning can help to differentiate tumor progression or recurrence from tumor pseudoprogression or radiation injuries.<sup>44</sup> Meta-analyses showed that sensitivity and specificity of [<sup>18</sup>F]FDG PET scans for distinction between WHO grade 3 and 4 gliomas progression versus treatment-related changes are 78% to 84% and 70% to 87%, respectively, with wide 95% confidence intervals (CI), especially in term of specificity.<sup>44–46</sup> The sensitivity of [<sup>18</sup>F]FDG PET/CT scanning is limited by the high [<sup>18</sup>F]FDG background uptake, especially when lesions are small ( $\leq 20$  mm in diameter) and located in the gray matter.<sup>47</sup> The specificity might be limited by inflammation, especially early after surgery and/or radiation therapy. Again, the combined use of multiparametric MRI and [<sup>18</sup>F]FDG provides higher accuracy, in particular when including information provided by perfusion MRI.<sup>48,49</sup>

## RADIOLABELED AMINO ACIDS

An alternate metabolic pathway was investigated when the radiolabeled AA, L-methyl-[<sup>11</sup>C]methionine ([<sup>11</sup>C]MET) was developed in the 1980s.<sup>50</sup> L-type AAs are actively transported from systemic circulation across the BBB into the brain by L-type AA transporter 1 (LAT1) expressed in luminal and abluminal sides of the BBB endothelial cells.<sup>51</sup> The L-type AAs are, therefore, transported in normal brain and brain lesions without BBB disruption such as WHO grade 2 gliomas.<sup>52</sup> By contrast with [<sup>18</sup>F]FDG PET scans, the radiolabeled [<sup>11</sup>C]MET PET images show a low background activity in normal brain, providing higher tumor-to-background contrast, even in low-grade gliomas.<sup>53</sup> LAT1 is expressed by endothelial cells and tumor cells, and the high AAs transport in higher grade gliomas and brain metastases might be related to increased microvessel density (angiogenesis) and/or increased tumor cell density and/or LAT1 overexpression and transport activity, ultimately reflecting tumor cells proliferation activity.<sup>54–56</sup> The sensitivity and specificity of [<sup>11</sup>C]MET PET for the diagnosis of suspected glioma are variable, at 76% to 100% and 75% to 100%, respectively.<sup>56</sup> Some WHO grade 2 gliomas show no [<sup>11</sup>C]MET uptake, resulting in false-negative results.<sup>56,57</sup> Similar to [<sup>18</sup>F]FDG, false-positive cases have been reported using [<sup>11</sup>C]MET PET due to uptake in inflammatory

processes and treatment-related changes owing to BBB disruption and vascular proliferation, including leucoencephalitis, brain abscesses, multiple sclerosis, hematoma, necrosis, acute demyelination, and ischemia.<sup>56,58–61</sup> The WHO grade 3 and 4 gliomas are more likely to show higher [<sup>11</sup>C]MET uptake than WHO grade 2 gliomas.<sup>56</sup> Various TBR cutoff values, ranging from 1.3 to 2.05, have been used to predict glioma grade using [<sup>11</sup>C]MET PET, providing limited accuracy as a consequence of a large TBR values overlaps between WHO grade 2, 3, and 4 gliomas.<sup>56</sup> Similar to [<sup>18</sup>F]FDG, high [<sup>11</sup>C]MET TBR have been reported in oligodendrogiomas with 1p/19q codeletion, as high as in WHO grade 3 and 4 gliomas.<sup>31,53</sup> Overall, areas of highest [<sup>18</sup>F]FDG uptake and [<sup>11</sup>C]MET uptake are concordant in gliomas; however, owing to the low background activity using [<sup>11</sup>C]MET PET scans, the latter is preferred for guiding biopsy, but also to better delineate tumor extent for radiation therapy planning.<sup>37,62</sup>

The drawbacks of PET imaging using [<sup>11</sup>C]MET are many, including the short half-life of [<sup>11</sup>C] (20 minutes) requiring on-site cyclotron, and the rapid incorporation after a few minutes of [<sup>11</sup>C]MET into proteins and tracer metabolism into radiolabeled metabolites.<sup>63</sup> Therefore, in the 1990s, the [<sup>18</sup>F]-labeled artificial AA, O-(2-[<sup>18</sup>F]fluoroethyl)-L-tyrosine (<sup>18</sup>F)FET, was developed with the advantages of the longer half-life of [<sup>18</sup>F] (110 minutes) and of not being incorporated into proteins, resulting in the absence of radiolabeled metabolites.<sup>64,65</sup> Owing to its low lipophilicity, brain [<sup>18</sup>F]FET uptake by diffusion through the BBB is not significant.<sup>64</sup> Another advantage of [<sup>18</sup>F]FET is its lower uptake in inflammatory cells compared with [<sup>11</sup>C]MET.<sup>58,59</sup> Similar clinical performances are reported for [<sup>11</sup>C]MET and [<sup>18</sup>F]FET in the management of gliomas and metastases.<sup>66</sup> In a meta-analysis assessing the diagnostic performance of [<sup>18</sup>F]FET and [<sup>18</sup>F]FDG PET in suspected brain tumors, Dunet and colleagues<sup>32</sup> demonstrated a significantly higher sensitivity of [<sup>18</sup>F]FET PET (0.94; 95% CI, 0.79–0.98) compared with [<sup>18</sup>F]FDG (0.38; 95% CI, 0.27–0.50) for the diagnosis of brain tumor versus nontumoral lesions, with comparable specificity (0.88; 95% CI, 0.37–0.99, and 0.86; 95% CI, 0.31–0.99, respectively). Even though [<sup>18</sup>F]FET is transported in gliomas irrespective of BBB disruption, passive tracer influx through disrupted BBB disruption, passive tracer influx through disrupted BBB and in non-neoplastic brain lesions limits the specificity of [<sup>18</sup>F]FET.<sup>67</sup> As with [<sup>18</sup>F]FDG and [<sup>11</sup>C]MET PET, [<sup>18</sup>F]FET PET can be falsely positive in brain abscesses, intracerebral acute hematomas, acute infarctions, demyelinating inflammatory central

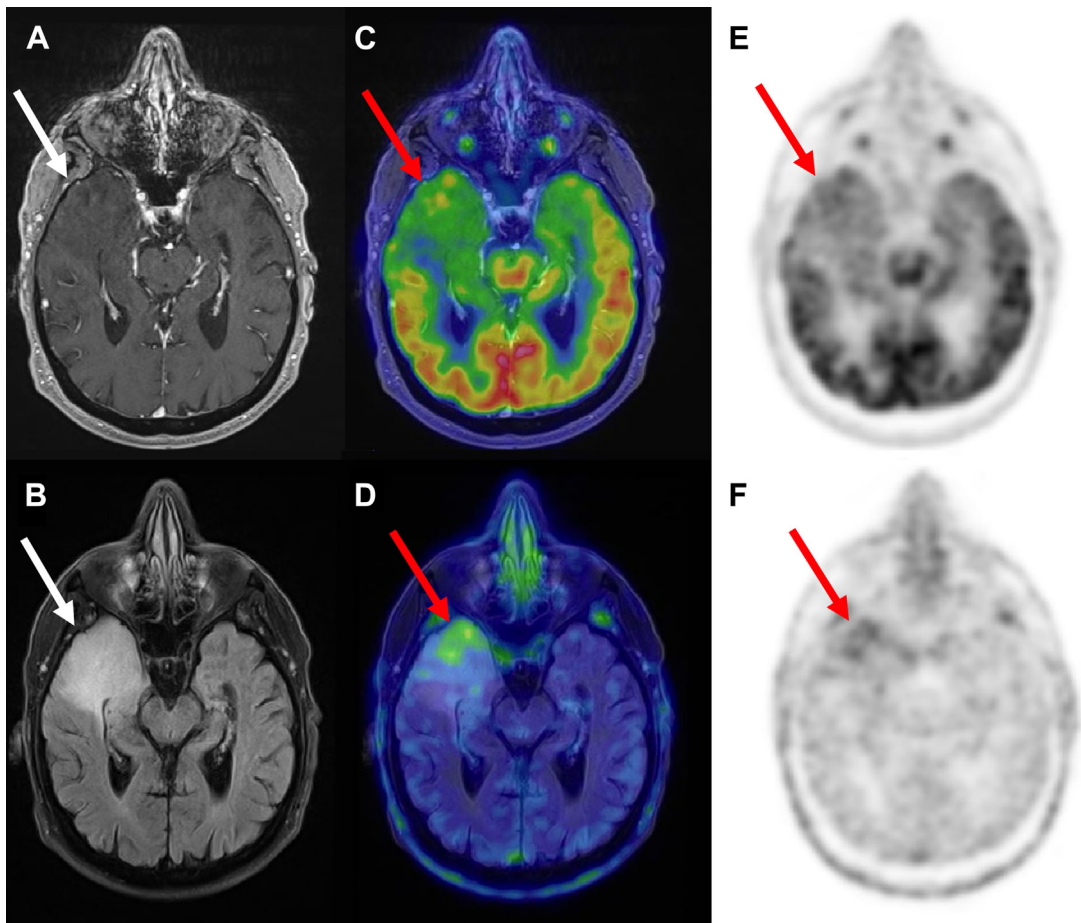


**Fig. 3.** Brain images of a 73-year-old patient with clinical presentation of new-onset epilepsy. The MRI showed a right temporal lesion with mild enhancement (*A*, postgadolinium T1-weighted sequence; *B*, T2-weighted/fluid-attenuated inversion recovery [FLAIR] MR image; white arrows). The [<sup>18</sup>F]FDG PET scan showed tumoral uptake lower than gray matter (*C*, fused PET/MRI; *E*, PET image SUV scale 0–8; TBR<sub>max</sub> 0.7; red arrows). The [<sup>18</sup>F]FET PET scan showed a heterogeneous lesion with foci of higher [<sup>18</sup>F]FET uptake (*D*, fused PET/MRI; *F*, PET image SUV scale 0–5; TBR<sub>max</sub> 2.8; red arrows). The pathologic analyses showed a WHO grade 4 glioma, *IDH* wild type.

nervous system lesions (eg, multiple sclerosis), meningoencephalitis, and other conditions with acute inflammation and/or reactive astrogliosis.<sup>33,59,67,68</sup> Both [<sup>18</sup>F]FDG and radiolabeled AAs PET can also be falsely positive in (neuro)sarcoidosis.<sup>67,69</sup> In addition, high [<sup>18</sup>F]FET activity can be observed in vascular malformations, including cavernoma.<sup>67</sup> [<sup>11</sup>C]MET and [<sup>18</sup>F]FET uptake mimicking tumor activity has been reported in (subclinical) epileptic activity associated with brain tumors, radiation necrosis, focal cortical dysplasia, or arteriovenous malformations.<sup>70–73</sup> In contrast, the negative predictive value of [<sup>18</sup>F]FET PET to exclude gliomas is limited because [<sup>18</sup>F]FET PET scans can be negative in about 30% of WHO grade 2 gliomas.<sup>73–75</sup> Nevertheless, a negative [<sup>18</sup>F]FET PET scans excludes WHO grade 3 and 4 gliomas with a high probability

(with the exception for small lesions).<sup>73,75</sup> [<sup>18</sup>F]FET PET scans actually identify WHO grade 3 and 4 gliomas in up to one-third of the patients whose preoperative MRI suspected WHO grade 2 glioma, with a sensitivity of 95%, specificity of 72%, positive predictive value of 74%, and negative predictive value of 95%.<sup>62,76,77</sup> The radiolabeled AAs PET, thanks to the lower background activity compared with [<sup>18</sup>F]FDG, can better identify the most appropriate site of biopsy in heterogeneous lesions, detecting foci of higher grade gliomas with no or mild contrast enhancement in MR images, avoiding biopsy undersampling (Fig. 3).<sup>19</sup> Similar to [<sup>11</sup>C]MET, there are large overlaps in TBR values across WHO grade 2, 3, and 4 gliomas (see Fig. 1).<sup>73</sup> However, the accuracy to distinguish WHO grade 2 from WHO grade 3 and 4 gliomas is improved when evaluating the kinetics

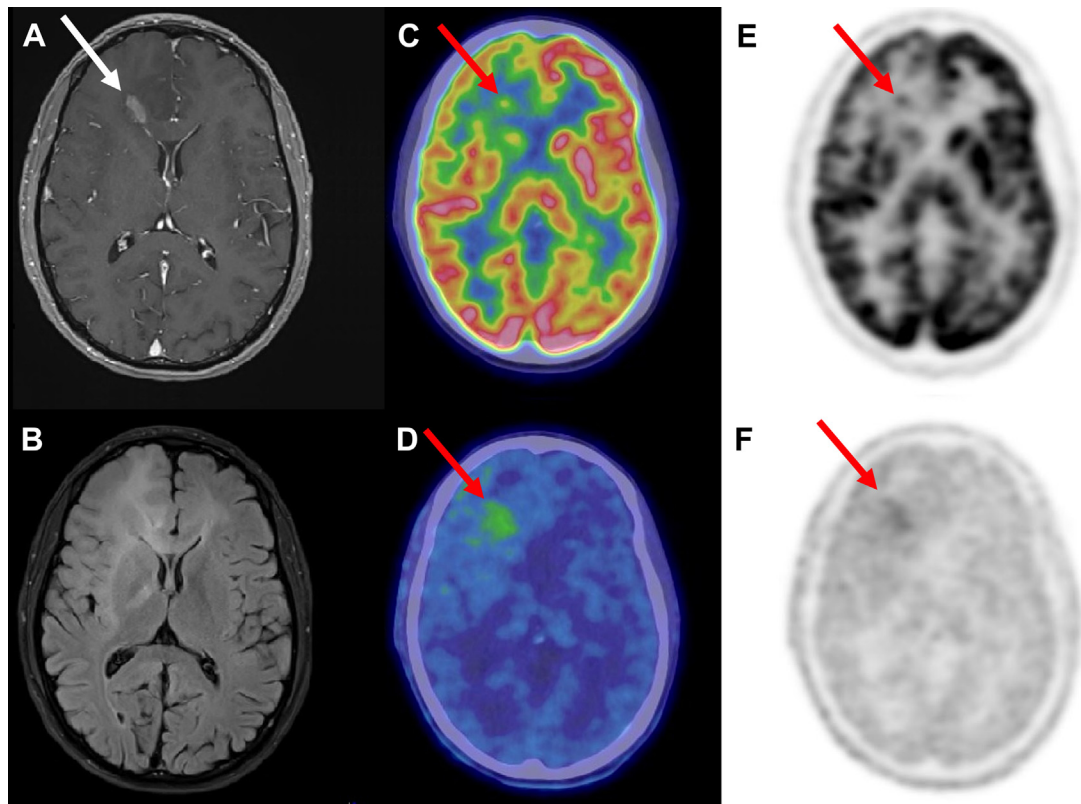


**Fig. 4.** Brain images of a 25-year-old patient with the initial diagnosis of WHO grade 2 diffuse astrocytoma located in the right frontal lobe, who underwent maximal surgical resection. Five years later, a follow-up MRI showed the appearance of a focal area of gadolinium enhancement in T1-weighted sequence (A, T1-weighted sequence, white arrow; B, T2/fluid-attenuated inversion recovery [FLAIR] sequence). The  $[^{18}\text{F}]$ FDG PET images (C, fused PET/MRI; E, PET image SUV scale 0–8; red arrows) showed a focal high uptake corresponding to the gadolinium enhancement with  $\text{TBR}_{\max}$  estimated at 0.6, suggesting malignant transformation. The  $[^{18}\text{F}]$ FET PET images (D, fused PET/MRI; F, PET image SUV scale 0–5; red arrows) showed larger extent of uptake and a slightly higher uptake in the same region as  $[^{18}\text{F}]$ FDG PET scan and MRI with a  $\text{TBR}_{\max}$  estimated at 2.6. Note that  $2-[^{18}\text{F}]$ fluoro-L-tyrosine ( $[^{18}\text{F}]$ TYR) did not show tumoral uptake at diagnosis (image not showed). Pathology confirmed transformation into WHO grade 3 glioma.

of  $[^{18}\text{F}]$ FET uptake. Indeed, the time–activity curves increase for WHO grade 2 gliomas, and decrease for WHO grade 3 and 4 gliomas, with the early timeframe (5–15 minutes) showing the greater difference.<sup>27,62,75,78,79</sup> The biological processes underlying  $[^{18}\text{F}]$ FET time–activity curve patterns are not yet elucidated and the contribution of  $[^{18}\text{F}]$ FET transport activity, blood volume and perfusion (related to increased angiogenesis in WHO grade 4 gliomas), possible passive diffusion in disrupted BBB in WHO grade 3 and 4 gliomas and  $[^{18}\text{F}]$ FET efflux, respectively, is not known.<sup>80,81</sup> Even if the kinetic parameters are taken into account,  $[^{18}\text{F}]$ FET PET scanning has limited accuracy to predict glioma grade at diagnosis, as well as detecting malignant transformation of WHO grade 2 gliomas.<sup>82,83</sup> **Fig. 4** illustrates a case for which both  $[^{18}\text{F}]$ FET PET and  $[^{18}\text{F}]$ FDG PET scans were performed for a

suspected malignant transformation of a WHO grade 2 diffuse astrocytoma; the  $[^{18}\text{F}]$ FDG PET scan alone correctly detected malignant transformation to WHO grade 3 glioma. However, the  $[^{18}\text{F}]$ FET PET scan allowed better delineation of tumor recurrence extent, which might be a valuable complementary information for surgical planning.

The undisputed advantage of radiolabeled AAs over  $[^{18}\text{F}]$ FDG is the better contrast between tumor uptake and cortical background, making possible the delineation of tumor extent, helping radiation oncologist for tumor delineation, especially beyond contrast-enhanced areas for which MRI has a limited ability to differentiate nonenhancing infiltrating tumor from edema or treatment-related changes in cases of recurrence.<sup>36,84–89</sup> A large retrospective multicenter study showed an association between overall survival and maximal resection of both contrast-

enhanced and non-contrast-enhanced tumor using MRI in patients with newly diagnosed WHO grade 4 glioma regardless of *IDH* status, and methylation status of the *MGMT* promoter in patients with *IDH* wild-type WHO grade 4 glioma.<sup>90</sup> Baseline tumor volume based on [<sup>18</sup>F]FET PET scans in patients with newly diagnosed WHO grade 4 glioma before radiotherapy plus concomitant and adjuvant temozolomide was inversely correlated with progression-free survival and overall survival.<sup>91</sup> [<sup>18</sup>F]FET PET scanning might be of interest for surgical resection planning with the aim to increase the chances of maximal resection, in combination with preoperative MRI and using 5-aminolevulinic acid for the intraoperative visualization of areas of tumor infiltration.<sup>92–94</sup>

During the first 3 months after chemoradiotherapy completion in case WHO grade 4 gliomas, when pseudoprogression is suspected, radiolabeled AAs PET has an added value when perfusion MRI is not conclusive.<sup>36</sup> The accuracy of [<sup>18</sup>F]FET PET scanning in differentiating recurrent WHO grade 4 gliomas from post-treatment changes is high, with sensitivities ranging from 82% to 100% and specificities from 86% to 94%.<sup>95–99</sup> In a recent study including patients with WHO grade 4 gliomas treated with lomustine–temozolomide chemoradiation and for which MRI was equivocal after radiotherapy inside the radiation field (median time interval, 10 weeks; range, 5–34 weeks), [<sup>18</sup>F]FET PET imaging proved highly performant using a TBR<sub>mean</sub> cutoff of less than 1.95 (sensitivity, 82%; specificity, 92%; positive predictive value, 90%; negative predictive value, 85%; accuracy, 87%; area under the curve  $\pm$  standard error, 0.77  $\pm$  0.12).<sup>95</sup> When radiation necrosis is suspected in case of gliomas or metastases, radiolabeled AAs PET may help when perfusion MRI is uncertain.<sup>36,42</sup> However, the accuracy varies across studies (sensitivity of 74%–90%; specificity of 73%–100%); false-positive and false-negative results can occur, depending on tumor cell type and LAT activity, tracer activity related to passive diffusion across disrupted BBB and vascular volume and density associated with angiogenesis (Fig. 5).<sup>42,100</sup>

The AA 3, 4-dihydroxy-6-[<sup>18</sup>F]-fluoro-L-phenylalanine ([<sup>18</sup>F]DOPA) has also been used for imaging brain tumors; it is also transported across the BBB and in tumor cells by LAT and [<sup>18</sup>F]DOPA PET showed comparable performances to [<sup>18</sup>F]FET and [<sup>11</sup>C]MET PET scanning.<sup>45,46,45</sup> One limitation of [<sup>18</sup>F]DOPA is that it is rapidly metabolized in the periphery and in the striatum, and released [<sup>18</sup>F]-labeled metabolites can be transported again and cross the BBB.<sup>101–103</sup> Tatekawa and

colleagues<sup>104</sup> recently showed a relationship between [<sup>18</sup>F]DOPA uptake and ADC and rCBV measurements, respectively, in different molecular subtypes of gliomas. The [<sup>18</sup>F]DOPA SUV normalized to the median uptake value of the striatum was positively correlated with rCBV and negatively correlated with ADC in *IDH* wild-type and *IDH* mutant 1p/19q noncodeleted gliomas, whereas a significant positive correlation was observed between the SUV normalized to the median uptake value of the striatum and the ADC only in the subgroup of oligodendroglomas with *IDH* mutant and 1p/19q codeletion.<sup>104</sup>

For the distinction between true recurrence and radiation necrosis in a small patients sample, Jena and colleagues<sup>105</sup> recently showed that the combination [<sup>18</sup>F]DOPA PET imaging of multiparametric MRI (perfusion, diffusion, and spectroscopy) achieved 95% accuracy with greater than 95% sensitivity and specificity.

The non-natural AA anti-1-amino-3-[<sup>18</sup>F]fluorocyclobutane-1-carboxylic acid ([<sup>18</sup>F]FACBC), originally developed for brain tumor imaging has been less investigated.<sup>106</sup> By contrast with [<sup>11</sup>C]MET, [<sup>18</sup>F]FET, and [<sup>18</sup>F]DOPA, the transport of [<sup>18</sup>F]FACBC across the BBB and in tumor cells is mediated mainly by the alanine, serine, cysteine transporter 2 (ASCT2; SLC1A5).<sup>107</sup> Michaud and colleagues<sup>107</sup> showed lower and slower uptake of [<sup>18</sup>F]FACBC than [<sup>11</sup>C]MET in brain lesions suspected of glioma recurrence or progression, although the [<sup>18</sup>F]FACBC normal brain background was lower.

## NON-AMINO ACID POSITRON EMISSION TOMOGRAPHY RADIOTRACERS

Similar to AAs, non-AAs unconventional tracers providing low or no background activity in brain compared with [<sup>18</sup>F]FDG and better contrast, are being investigated for glioma imaging.<sup>108</sup> The delivery of an imaging agent into the brain is challenged by highly restricted BBB.<sup>109</sup> After intravenous injection, for the tracer to reach brain tumor cells, when the BBB is intact, it must first be recognized by a receptor on the BBB (the imaging agent should mimic the structure of transporter substrate), be transported in luminal and abluminal sides of the BBB endothelial cells and reach the tumor cell target after entering into the brain parenchyma, and, ultimately, in a sufficient amount to obtain a detectable imaging signal.<sup>110</sup> For example, the promising radiolabeled ligand targeting fibroblast activation protein [<sup>68</sup>Ga]FAPI, shows high accumulation in *IDH*-wildtype WHO 4 gliomas and WHO grade 3 and 4 gliomas, with a disrupted BBB, but not in WHO grade II gliomas. It is highly

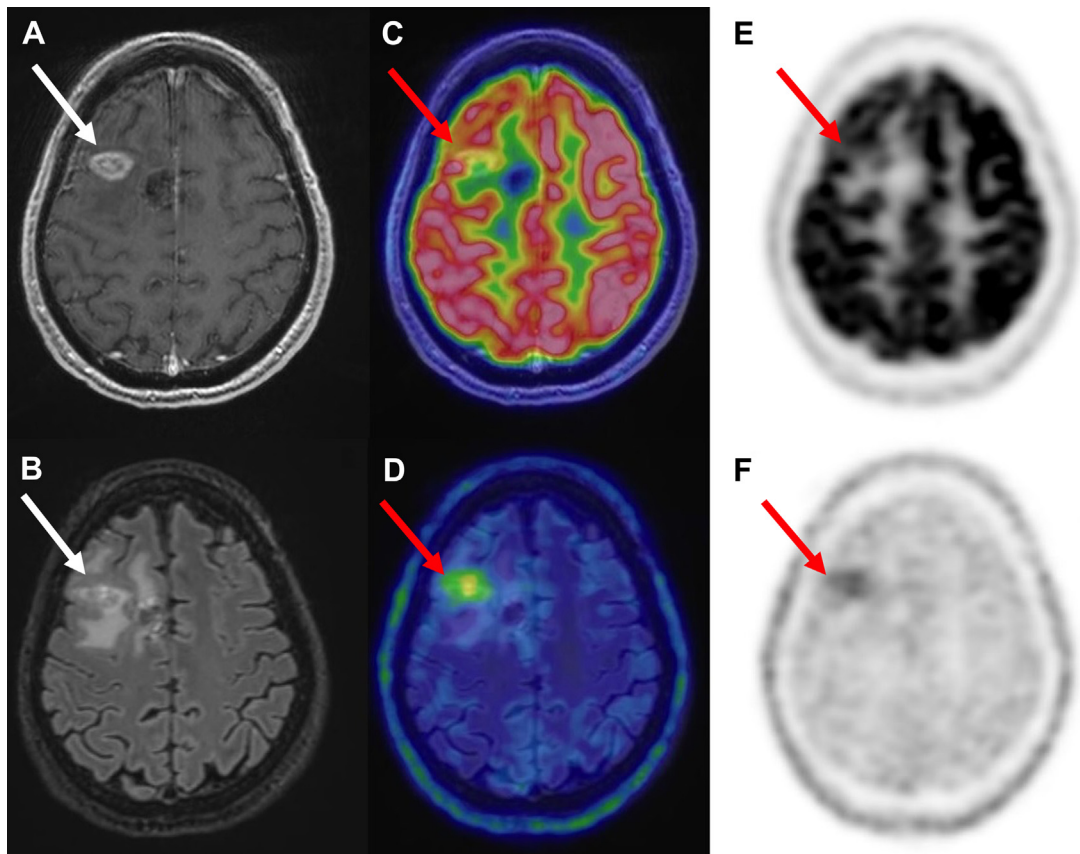


**Fig. 5.** Brain Images of a 65-year-old patient with a WHO grade 4 glioma with MGMT promoter methylation and suspected recurrence 4 months after the end of concomitant radiochemotherapy based on follow-up multiparametric MRI (*A*, postgadolinium T1-weighted sequence; *B*, T2/fluid-attenuated inversion recovery [FLAIR] MRI; white arrows) showing an area of gadolinium enhancement with increased rCBV (perfusion MRI not shown) next to surgical resection site in the right frontal lobe. The  $[^{18}\text{F}]$ FDG PET/CT scan did not show  $[^{18}\text{F}]$ FDG uptake higher than gray matter (*C*, fused PET/MRI; *E*, PET image, SUV scale 0–8; red arrows). The  $[^{18}\text{F}]$ FET PET images (*D*, fused PET/MRI; *F*, PET image, SUV scale 0–5; red arrows) showed  $[^{18}\text{F}]$ FET uptake with the TBR<sub>max</sub> estimated at 3.2 suggesting glioma recurrence. The lesion was resected, and the pathologic analyses showed radiation necrosis.

probable that it is not transported across an intact BBB, which in all likelihood will limit its clinical use for brain tumors.<sup>111</sup> Moreover, the BBB expresses efflux transporters, such as P-glycoprotein, to prevent drugs entering into the brain parenchyma, exporting them from endothelial cells back into circulating blood.<sup>109</sup> This efflux can occur with radiolabeled AAs such as  $[^{18}\text{F}]$ FET and  $[^{11}\text{C}]$ MET and  $[^{11}\text{C}]$ -labeled metabolites, being responsible for the decrease of PET signal with time.<sup>80</sup>

Many non-AAs PET tracers showed uptake in gliomas, but the PET signal is often not related solely to the glioma tumor cells. The mitochondrial translocator protein 18 kDa (TSPO) is upregulated in glioma cells and might be a target of interest for gliomas imaging; however, radiolabeled ligands of TSPO were originally developed for neuroinflammation imaging, because TSPO is upregulated in

activated microglia and macrophages, thereby limiting the specificity of PET signal in glioma imaging.<sup>112</sup> Radiolabeled ligands of the prostate-specific membrane antigen PET/CT scans showed a high uptake in WHO grade 3 and 4 gliomas and might be used to differentiate WHO grade 3 and 4 from grade 2 gliomas, but the signal is mainly related to prostate-specific membrane antigen overexpression by activated endothelial cells of angiogenesis.<sup>113–116</sup> Similarly, WHO grade 4 gliomas showed uptake of the radiolabeled glycine–aspartic acid peptide  $[^{18}\text{F}]$ FPPRGD<sub>2</sub> targeting integrin  $\alpha_v\beta_3$ , not only owing to overexpression by glioma cells, but mainly related to integrin  $\alpha_v\beta_3$  upregulation in activated endothelial cells of glioma neovasculature.<sup>117</sup> The radiolabeled ligands of the chemokine receptor 4 allows for imaging of glioma cells as well as-tumor associated

neovasculature and immune cells of tumor microenvironment.<sup>118</sup>

Even though non-AA tracers are not specific for tumor cells imaging, they might still be used to better delineate tumor extent and, more importantly, being used as radiotheranostic agents.<sup>119</sup>

## DISCUSSION

Radiolabeled AAs and singularly [<sup>18</sup>F]FET, developed more recently than [<sup>18</sup>F]FDG, have gained wider clinical acceptance, and this was translated into official recommendations by the Response Assessment in Neuro-Oncology working group and European Association for Neuro-Oncology, who concluded in 2016 regarding the “superiority of AA PET over glucose PET.”<sup>119</sup> It is obvious that [<sup>18</sup>F]FET brings highly valuable information in several indications, but, in our opinion, it is more a matter of when to combine [<sup>18</sup>F]FET with [<sup>18</sup>F]FDG, rather than replacing one with another.

When it comes to distinguish neoplastic from non-neoplastic brain lesions, as well as predict glioma WHO grade, both [<sup>18</sup>F]FDG and radiolabeled AAs present clinical limitations. In both cases, there are overlaps in the tracer uptake intensity across WHO grades 2, 3 and 4, especially in gliomas with an oligodendroglial component.<sup>31,32,61,67,73</sup> A shift toward using AAs has been advocated, notably based on a meta-analysis performed by Dunet and colleagues<sup>32</sup> in 2016. It compared the diagnostic performances of [<sup>18</sup>F]FDG and [<sup>18</sup>F]FET, based on a direct comparison of both tracers in the all patients and with histology as reference standard.<sup>32</sup> The performance of [<sup>18</sup>F]FDG PET scanning for the diagnosis of brain tumor was significantly lower than [<sup>18</sup>F]FET PET scanning (area under the curve, 0.56 [95% CI, 0.47–0.66] and 0.85 [95% CI, 0.77–0.93], respectively;  $P<.0001$ ). Concluding to the definite superiority of [<sup>18</sup>F]FET over [<sup>18</sup>F]FDG in this setting would be misleading, however, considering the small number of studies (5 papers published between 2006 and 2010) and patients ( $n = 119$  patients:  $n = 82$  gliomas;  $n = 8$  nonglioma tumors, and  $n = 29$  nontumoral lesions). In addition to the sample size, variations in patient selection and imaging procedures are such as it would not be reasonable to generalize the conclusions.<sup>32,120</sup>

Several meta-analyses looked at the performances of the various radiotracers to assess tumor recurrence and progression after treatment, including radiation therapy. Nihashi and colleagues<sup>44</sup> showed in 2013 for [<sup>18</sup>F]FDG and [<sup>11</sup>C]MET a pooled sensitivity of 0.79 (0.67–0.88) and 0.70 (0.50–0.84), respectively, and a specificity of

0.70 (0.50–0.84) and 0.93 (0.44–1.0), respectively. More recently, de Zwart and colleagues<sup>45</sup> showed for [<sup>18</sup>F]FDG, [<sup>18</sup>F]FET, and [<sup>11</sup>C]MET sensitivities of 0.82 (0.64–0.92), 0.90 (0.81–0.95), and 0.91 (0.78–0.97), respectively, and specificities of 0.79 (0.61–0.90), 0.85 (0.71–0.93), and 0.83 (0.68–0.92), respectively. Cui and colleagues, evaluated all 4 available tracers in 2021, and found a somewhat lower sensitivity of [<sup>18</sup>F]FDG PET scanning with a pooled value of 0.76 (0.68–0.83) compared with radiolabeled AAs ([<sup>18</sup>F]FET: 0.88, [<sup>18</sup>F]DOPA: 0.85, and [<sup>11</sup>C]MET: 0.92). However, [<sup>18</sup>F]FDG PET scanning recorded the highest specificity with a pooled value of 0.87 (0.70–0.90), compared with 0.78, 0.70, and 0.78 for the 3 AAs, respectively.<sup>46</sup> A systematic review by Furuse and colleagues<sup>121</sup> further suggests that [<sup>18</sup>F]FDG PET provides higher accuracy to differentiate radiation necrosis from tumor progression in patients with metastatic brain tumors than in patients with gliomas.

In this indication, and similar to the initial diagnosis setting, the picture as to which radiotracer should be preferred as a first-line PET is not as clear cut as it may seem. At the very least, [<sup>18</sup>F]FDG is not thoroughly outperformed and surely cannot be discarded altogether.

Prognostic factors associated with progression-free survival and overall survival of patients with gliomas include age, tumor diameter, tumor crossing midline, performance status, and the molecular subgroup (eg, among patients with WHO grade 2 and 3 gliomas, IDH wild-type group is associated with the worst prognosis), and the extent of tumor debulking when maximal resection is possible.<sup>7</sup> Both [<sup>18</sup>F]FDG and radiolabeled AA PET scans might provide independent prognostic information, such as the baseline metabolic tumor volume assessed using AAs PET scans and the extent of residual tumor early after surgery before radiation therapy.<sup>35,88,91,122–126</sup>

Despite the vastness of the available literature dealing with PET/CT scans or PET/MRI in brain tumors, these studies are often limited by the retrospective design and/or the small patient sample. Moreover, patients’ selection criteria including the acquired sequences and results of multiparametric MRI may vary; the population of interest might also be heterogeneous as studies were performed before the latest updates of WHO CNS5 molecular classification published in 2021.<sup>3</sup> Eventually, the reference standard is most of the time based on imaging follow-up. Furthermore, despite valuable attempts by the European Association of Nuclear Medicine, the Society of Nuclear Medicine and Molecular Imaging, the European Association of Neuro-oncology, and the working group for

Response Assessment in Neuro-oncology with PET (PET-Response Assessment in Neuro-Oncology working group), there is not a single well-defined method that would consistently provide high diagnostic accuracy in the clinical setting (eg, various TBR<sub>max</sub> and TBR<sub>mean</sub> cutoff values based on early static vs kinetic parameters are proposed for [<sup>18</sup>F]FET PET depending on clinical question).<sup>27</sup> Harmonization and prospective validation of PET image interpretation criteria should improve the interobserver agreement and facilitate comparison of studies results in literature. Future prospective studies should clarify the performance of [<sup>18</sup>F]FDG PET scans and radiolabeled AA PET scans (and the combination) not in abstracto, but as a complementary tool to brain multiparametric MRI, taking into account the molecular profile of gliomas presented in the WHO CNS5 classification.<sup>3</sup> The past few years have witnessed major improvements in PET/CT detectors and reconstruction algorithms, which have further improved image resolution and lesion detectability with reduced image noise. This should positively impact the diagnostic performances of PET scanning, especially using [<sup>18</sup>F]FDG as those images in which normal background is high.<sup>127</sup> Radiomics and artificial intelligence will certainly further enhance multimodality imaging performances; a recent review by Lohmann and colleagues<sup>128</sup> gives an overview of feature-based radiomics in neuro-oncology and examples of clinical applications.

The advantage of [<sup>18</sup>F]FDG over radiolabeled AAs is its wide availability and low cost. Therefore, when multiparametric MRI is not conclusive, [<sup>18</sup>F]FDG might be the first-choice PET tracer in cases of WHO grade 3 and 4 gliomas or [<sup>18</sup>F]FDG-avid tumors, avoiding the use of more expensive and less available radiolabeled AAs (eg, [<sup>11</sup>C]MET, [<sup>18</sup>F]FET, or [<sup>18</sup>F]DOPA). Radiolabeled AAs PET scans should be preferred in cases of WHO grade 2 gliomas or non [<sup>18</sup>F]FDG-avid tumors. Ultimately, [<sup>18</sup>F]FDG PET scans and radiolabeled AA PET scans can be combined together with multiparametric MRI to increase diagnostic confidence.<sup>13,129</sup>

## CLINICS CARE POINTS

- [<sup>18</sup>F]FDG PET/CT scanning is a widely accessible imaging method that may be helpful for characterizing suspicious MRI lesions.
- [<sup>18</sup>F]FDG PET/CT scanning performs fairly well for assessing the recurrence or persistence of high-grade gliomas.

- Tumor limits are more precisely delineated with [<sup>18</sup>F]FET and [<sup>18</sup>F]FDOPA than with [<sup>18</sup>F]FDG, including low-grade gliomas.
- [<sup>18</sup>F]FET PET scans can be falsely negative in up to 30% of WHO grade 2 gliomas.
- The specificity of AA PET scans is not perfect. Non-neoplastic brain conditions with increased blood flow and/or microvessel density, (sub-)acute inflammation or BBB disruption may all lead to false-positive results.
- Both [<sup>18</sup>F]FDG and radiolabeled AA PET scan performances should be further assessed, integrating gliomas molecular profile presented in the latest WHO CNS5 classification.

## DISCLOSURE

The authors received no financial support for the work, authorship, and/or publication of this article.

## REFERENCES

- Ostrom QT, Wright CH, Barnholtz-Sloan JS. Brain metastases: epidemiology. *Handb Clin Neurol* 2018;149:27–42.
- Miller KD, Ostrom QT, Kruchko C, et al. Brain and other central nervous system tumor statistics. *CA Cancer J Clin* 2021;71(5):381–406.
- Louis DN, Perry A, Wesseling P, et al. The 2021 WHO classification of tumors of the central nervous system: a summary. *Neuro Oncol* 2021;23(8):1231–51.
- Leeper HE, Caron AA, Decker PA, et al. IDH mutation, 1p19q codeletion and ATRX loss in WHO grade II gliomas. *Oncotarget* 2015;6(30):30295–305.
- Weller M, van den Bent M, Preusser M, et al. EANO guidelines on the diagnosis and treatment of diffuse gliomas of adulthood. *Nat Rev Clin Oncol* 2021;18(3):170–86.
- Ellingson BM, Wen PY, Cloughesy TF. Modified criteria for radiographic response assessment in glioblastoma clinical trials. *Neurotherapeutics* 2017;14(2):307–20.
- Nabors LB, Portnow J, Ahluwalia M, et al. Central nervous System Cancers, Version 3.2020, NCCN Clinical Practice Guidelines in Oncology. *J Natl Compr Canc Netw* 2020;18(11):1537–70.
- Le Rhun E, Guckenberger M, Smits M, et al. EANO-ESMO Clinical Practice Guidelines for diagnosis, treatment and follow-up of patients with brain metastasis from solid tumours. *Ann Oncol* 2021;32(11):1332–47.
- Wen PYC SM, Van den Bent MJ, Vogelbaum MA, et al. Response assessment in neuro-oncology clinical trials. *J Clin Oncol* 2017;35(21):2439–49.

10. Krabbe KG P, Wagn P, Hansen U, et al. MR diffusion imaging of human intracranial tumours. *Neuroradiology* 1997;39(7):483–9.
11. Hu R, Hoch MJ. Application of diffusion weighted imaging and diffusion tensor imaging in the pre-treatment and post-treatment of brain tumor. *Radiol Clin North Am* 2021;59(3):335–47.
12. Smits M. Imaging of oligodendrogloma. *Br J Radiol* 2016;89(1060):20150857.
13. Overcast WB, Davis KM, Ho CY, et al. Advanced imaging techniques for neuro-oncologic tumor diagnosis, with an emphasis on PET-MRI imaging of malignant brain tumors. *Curr Oncol Rep* 2021; 23(3):34.
14. Law M, Yang S, Wang H, et al. Glioma grading: sensitivity, specificity, and predictive values of perfusion MR imaging and proton MR spectroscopic imaging compared with conventional MR imaging. *AJNR Am J Neuroradiol* 2003;24(10): 1989–98.
15. van Dijken BRJ, van Laar PJ, Holtman GA, et al. Diagnostic accuracy of magnetic resonance imaging techniques for treatment response evaluation in patients with high-grade glioma, a systematic review and meta-analysis. *Eur Radiol* 2017;27(10): 4129–44.
16. Kaufmann TJ, Smits M, Boxerman J, et al. Consensus recommendations for a standardized brain tumor imaging protocol for clinical trials in brain metastases. *Neuro Oncol* 2020;22(6):757–72.
17. van Dijken BRJ, van Laar PJ, Smits M, et al. Perfusion MRI in treatment evaluation of glioblastomas: clinical relevance of current and future techniques. *J Magn Reson Imaging* 2019;49(1):11–22.
18. Thust SC, Heiland S, Falini A, et al. Glioma imaging in Europe: a survey of 220 centres and recommendations for best clinical practice. *Eur Radiol* 2018; 28(8):3306–17.
19. Albert NL, Weller M, Suchorska B, et al. Response Assessment in Neuro-Oncology working group and European Association for Neuro-Oncology recommendations for the clinical use of PET imaging in gliomas. *Neuro Oncol* 2016;18(9):1199–208.
20. Cooney TM, Cohen KJ, Guimaraes CV, et al. Response assessment in diffuse intrinsic pontine glioma: recommendations from the Response Assessment in Pediatric Neuro-Oncology (RAPNO) working group. *The Lancet Oncol* 2020;21(6): e330–6.
21. Fangusaro J, Witt O, Hernáiz Driever P, et al. Response assessment in paediatric low-grade glioma: recommendations from the Response Assessment in Pediatric Neuro-Oncology (RAPNO) working group. *The Lancet Oncol* 2020;21(6): e305–16.
22. Bi J, Chowdhry S, Wu S, et al. Altered cellular metabolism in gliomas - an emerging landscape of actionable co-dependency targets. *Nat Rev Cancer* 2020;20(1):57–70.
23. Borja AJ, Hancin EC, Raynor WY, et al. A critical review of PET tracers used for brain tumor imaging. *PET Clin* 2021;16(2):219–31.
24. Patching SG. Glucose transporters at the blood-brain barrier: function, regulation and gateways for drug delivery. *Mol Neurobiol* 2017;54(2): 1046–77.
25. Herholz K. Brain tumors: an update on clinical PET research in gliomas. *Semin Nucl Med* 2017;47(1): 5–17.
26. Flavahan WA, Wu Q, Hitomi M, et al. Brain tumor initiating cells adapt to restricted nutrition through preferential glucose uptake. *Nat Neurosci* 2013; 16(10):1373–82.
27. Law I, Albert NL, Arbizu J, et al. Joint EANM/EANO/RANO practice guidelines/SNMMI procedure standards for imaging of gliomas using PET with radio-labelled amino acids and [<sup>18</sup>F]FDG: version 1.0. *Eur J Nucl Med Mol Imaging* 2019;46(3):540–57.
28. Toyonaga T, Yamaguchi S, Hirata K, et al. Hypoxic glucose metabolism in glioblastoma as a potential prognostic factor. *Eur J Nucl Med Mol Imaging* 2017;44(4):611–9.
29. Delbeke D, Meyerowitz C, Lapidus RL, et al. Optimal cutoff levels of F-18 fluorodeoxyglucose uptake in the differentiation of low-grade from high-grade brain tumors with PET. *Radiology* 1995;195(1):47–52.
30. Borgwardt L, Hojgaard L, Carstensen H, et al. Increased fluorine-18 2-fluoro-2-deoxy-D-glucose (FDG) uptake in childhood CNS tumors is correlated with malignancy grade: a study with FDG positron emission tomography/magnetic resonance imaging coregistration and image fusion. *J Clin Oncol* 2005;23(13):3030–7.
31. Manabe O, Hattori N, Yamaguchi S, et al. Oligodendroglial component complicates the prediction of tumour grading with metabolic imaging. *Eur J Nucl Med Mol Imaging* 2015;42(6):896–904.
32. Dunet V, Pomoni A, Hottinger A, et al. Performance of <sup>18</sup>F-FET versus <sup>18</sup>F-FDG-PET for the diagnosis and grading of brain tumors: systematic review and meta-analysis. *Neuro Oncol* 2016;18(3): 426–34.
33. Cecchin D, Garibotto V, Law I, et al. PET imaging in neurodegeneration and neuro-oncology: variants and pitfalls. *Semin Nucl Med* 2021;51(5):408–18.
34. Krebs S, Mauguen A, Yildirim O, et al. Prognostic value of [<sup>18</sup>F]FDG PET/CT in patients with CNS lymphoma receiving ibrutinib-based therapies. *Eur J Nucl Med Mol Imaging* 2021;48(12):3940–50.
35. Chiang GC, Galla N, Ferraro R, et al. The added prognostic value of metabolic tumor size on FDG-PET at first suspected recurrence of glioblastoma multiforme. *J Neuroimaging* 2017;27(2):243–7.

36. Galldiks N, Niyazi M, Grosu AL, et al. Contribution of PET imaging to radiotherapy planning and monitoring in glioma patients - a report of the PET/RANO group. *Neuro Oncol* 2021;23(6):881–93.
37. Pirotte B, Goldman S, Massager N, et al. Comparison of <sup>18</sup>F-FDG and <sup>11</sup>C-methionine for PET-guided stereotactic brain biopsy of gliomas. *J Nucl Med* 2004;45(8):1293–8.
38. Pirotte BJ, Lubansu A, Massager N, et al. Clinical impact of integrating positron emission tomography during surgery in 85 children with brain tumors. *J Neurosurg Pediatr* 2010;5(5):486–99.
39. McCullough BJ, Ader V, Aguedan B, et al. Preoperative relative cerebral blood volume analysis in gliomas predicts survival and mitigates risk of biopsy sampling error. *J Neurooncol* 2018;136(1):181–8.
40. Petrella JR, Provenzale JM. MR perfusion imaging of the brain: techniques and applications. *AJR Am J Roentgenol* 2000;175(1):207–19.
41. Malani R, Bhatia A, Wolfe J, et al. Staging identifies non-CNS malignancies in a large cohort with newly diagnosed lymphomatous brain lesions. *Leuk Lymphoma* 2019;60(9):2278–82.
42. Galldiks N, Langen KJ, Albert NL, et al. PET imaging in patients with brain metastasis-report of the RANO/PET group. *Neuro Oncol* 2019;21(5):585–95.
43. Brandes AA, Franceschi E, Tosoni A, et al. MGMT promoter methylation status can predict the incidence and outcome of pseudoprogression after concomitant radiochemotherapy in newly diagnosed glioblastoma patients. *J Clin Oncol* 2008;26(13):2192–7.
44. Nihashi T, Dahabreh IJ, Terasawa T. Diagnostic accuracy of PET for recurrent glioma diagnosis: a meta-analysis. *AJNR Am J Neuroradiol* 2013;34(5):944–50. S941–S911.
45. de Zwart PL, van Dijken BRJ, Holtman GA, et al. Diagnostic Accuracy of PET tracers for the differentiation of tumor progression from treatment-related changes in high-grade glioma: a systematic review and metaanalysis. *J Nucl Med* 2020;61(4):498–504.
46. Cui M, Zorrilla-Veloz RI, Hu J, et al. Diagnostic accuracy of pet for differentiating true glioma progression from post treatment-related changes: a systematic review and meta-analysis. *Front Neurol* 2021;12:671867.
47. Dankbaar JW, Snijders TJ, Robe PA, et al. The use of (<sup>18</sup>)F-FDG PET to differentiate progressive disease from treatment induced necrosis in high grade glioma. *J Neurooncol* 2015;125(1):167–75.
48. Jena A, Taneja S, Jha A, et al. Multiparametric evaluation in differentiating glioma recurrence from treatment-induced necrosis using simultaneous (<sup>18</sup>)F-FDG-PET/MRI: a single-institution retrospective study. *AJNR Am J Neuroradiol* 2017;38(5):899–907.
49. Hojjati M, Badve C, Garg V, et al. Role of FDG-PET/MRI, FDG-PET/CT, and dynamic susceptibility contrast perfusion MRI in differentiating radiation necrosis from tumor recurrence in glioblastomas. *J Neuroimaging* 2018;28(1):118–25.
50. Lilja A, Bergstrom K, Hartvig P, et al. Dynamic study of supratentorial gliomas with L-methyl-<sup>11</sup>C-methionine and positron emission tomography. *AJNR Am J Neuroradiol* 1985;6(4):505–14.
51. Huttunen J, Peltokangas S, Gynther M, et al. L-Type Amino Acid Transporter 1 (LAT1/Lat1)-utilizing prodrugs can improve the delivery of drugs into neurons, astrocytes and microglia. *Sci Rep* 2019;9(1):12860.
52. Meyer GJ, Schober O, Hundeshagen H. Uptake of <sup>11</sup>C-L- and D-methionine in brain tumors. *Eur J Nucl Med* 1985;10(7–8):373–6.
53. Kim D, Chun JH, Kim SH, et al. Re-evaluation of the diagnostic performance of <sup>(11)C</sup>-methionine PET/CT according to the 2016 WHO classification of cerebral gliomas. *Eur J Nucl Med Mol Imaging* 2019;46(8):1678–84.
54. Okubo S, Zhen HN, Kawai N, et al. Correlation of L-methyl-<sup>11</sup>C-methionine (MET) uptake with L-type amino acid transporter 1 in human gliomas. *J Neurooncol* 2010;99(2):217–25.
55. Kracht LW, Friese M, Herholz K, et al. Methyl-[<sup>11</sup>C]-L-methionine uptake as measured by positron emission tomography correlates to microvessel density in patients with glioma. *Eur J Nucl Med Mol Imaging* 2003;30(6):868–73.
56. Glaudemans AW, Enting RH, Heesters MA, et al. Value of <sup>11</sup>C-methionine PET in imaging brain tumours and metastases. *Eur J Nucl Med Mol Imaging* 2013;40(4):615–35.
57. Herholz K, Holzer T, Bauer B, et al. <sup>11</sup>C-methionine PET for differential diagnosis of low-grade gliomas. *Neurology* 1998;50(5):1316–22.
58. Stober B, Tanase U, Herz M, et al. Differentiation of tumour and inflammation: characterisation of [<sup>3</sup>H]methylmethionine (MET) and O-(2-[<sup>18</sup>F]fluoroethyl)-L-tyrosine (FET) uptake in human tumour and inflammatory cells. *Eur J Nucl Med Mol Imaging* 2006;33(8):932–9.
59. Salber D, Stoffels G, Oros-Peusquens AM, et al. Comparison of O-(2-[<sup>18</sup>F]fluoroethyl)-L-tyrosine and L-<sup>3</sup>H-methionine uptake in cerebral hematomas. *J Nucl Med* 2010;51(5):790–7.
60. Nakajima R, Kimura K, Abe K, et al. <sup>11</sup>C-methionine PET/CT findings in benign brain disease. *Jpn J Radiol* 2017;35(6):279–88.
61. Van Laere K, CeysSENS S, Van Calenbergh F, et al. Direct comparison of <sup>18</sup>F-FDG and <sup>11</sup>C-methionine PET in suspected recurrence of glioma: sensitivity, inter-observer variability and prognostic

- value. *Eur J Nucl Med Mol Imaging* 2005;32(1):39–51.
62. Jansen NL, Graute V, Armbruster L, et al. MRI-suspected low-grade glioma: is there a need to perform dynamic FET PET? *Eur J Nucl Med Mol Imaging* 2012;39(6):1021–9.
  63. Ishiwata K, Vaalburg W, Elsinga PH, et al. Comparison of L-[1-11C]methionine and L-methyl-[11C] methionine for measuring *in vivo* protein synthesis rates with PET. *J Nucl Med* 1988;29(8):1419–27.
  64. Wester HJ, Herz M, Weber W, et al. Synthesis and radiopharmacology of O-(2-[18F]fluoroethyl)-L-tyrosine for tumor imaging. *J Nucl Med* 1999;40(1):205–12.
  65. Heiss P, Mayer S, Herz M, et al. Investigation of transport mechanism and uptake kinetics of O-(2-[18F]fluoroethyl)-L-tyrosine *in vitro* and *in vivo*. *J Nucl Med* 1999;40(8):1367–73.
  66. Grosu AL, Astner ST, Riedel E, et al. An interindividual comparison of O-(2-[18F]fluoroethyl)-L-tyrosine (FET)- and L-[methyl-11C]methionine (MET)-PET in patients with brain gliomas and metastases. *Int J Radiat Oncol Biol Phys* 2011;81(4):1049–58.
  67. Hutterer M, Nowosielski M, Putzer D, et al. [18F]-fluoro-ethyl-L-tyrosine PET: a valuable diagnostic tool in neuro-oncology, but not all that glitters is glioma. *Neuro Oncol* 2013;15(3):341–51.
  68. Lohaus N, Mader C, Jelcic I, et al. Acute Disseminated Encephalomyelitis in FET PET/MR. *Clin Nucl Med* 2022;47(2):e137–9.
  69. Yamada Y, Uchida Y, Tatsumi K, et al. Fluorine-18-fluorodeoxyglucose and carbon-11-methionine evaluation of lymphadenopathy in sarcoidosis. *J Nucl Med* 1998;39(7):1160–6.
  70. Sasaki M, Ichiya Y, Kuwabara Y, et al. Hyperperfusion and hypermetabolism in brain radiation necrosis with epileptic activity. *J Nucl Med* 1996;37(7):1174–6.
  71. Sasaki M, Kuwabara Y, Yoshida T, et al. Carbon-11-methionine PET in focal cortical dysplasia: a comparison with fluorine-18-FDG PET and technetium-99m-ECD SPECT. *J Nucl Med* 1998;39(6):974–7.
  72. Hutterer M, Ebner Y, Riemenschneider MJ, et al. Epileptic activity increases cerebral amino acid transport assessed by 18F-Fluoroethyl-L-Tyrosine amino acid PET: a potential brain tumor mimic. *J Nucl Med* 2017;58(1):129–37.
  73. Rapp M, Heinzel A, Galldiks N, et al. Diagnostic performance of 18F-FET PET in newly diagnosed cerebral lesions suggestive of glioma. *J Nucl Med* 2013;54(2):229–35.
  74. Floeth FW, Pauleit D, Sabel M, et al. Prognostic value of O-(2-18F-fluoroethyl)-L-tyrosine PET and MRI in low-grade glioma. *J Nucl Med* 2007;48(4):519–27.
  75. Albert NL, Winkelmann I, Suchorska B, et al. Early static (18)F-FET-PET scans have a higher accuracy for glioma grading than the standard 20–40 min scans. *Eur J Nucl Med Mol Imaging* 2016;43(6):1105–14.
  76. Ewelt C, Floeth FW, Felsberg J, et al. Finding the anaplastic focus in diffuse gliomas: the value of Gd-DTPA enhanced MRI, FET-PET, and intraoperative, ALA-derived tissue fluorescence. *Clin Neurosurg* 2011;113(7):541–7.
  77. Scott JN, Brasher PM, Sevick RJ, et al. How often are nonenhancing supratentorial gliomas malignant? A population study. *Neurology* 2002;59(6):947–9.
  78. Popperl G, Kreth FW, Mehrkens JH, et al. FET PET for the evaluation of untreated gliomas: correlation of FET uptake and uptake kinetics with tumour grading. *Eur J Nucl Med Mol Imaging* 2007;34(12):1933–42.
  79. Langen KJ, Stoffels G, Filss C, et al. Imaging of amino acid transport in brain tumours: positron emission tomography with O-(2-[(18)F]fluoroethyl)-L-tyrosine (FET). *Methods* 2017;130:124–34.
  80. Richard MA, Fouquet JP, Lebel R, et al. Determination of an Optimal Pharmacokinetic Model of (18)F-FET for quantitative applications in rat brain tumors. *J Nucl Med* 2017;58(8):1278–84.
  81. Gottler J, Lukas M, Kluge A, et al. Intra-lesional spatial correlation of static and dynamic FET-PET parameters with MRI-based cerebral blood volume in patients with untreated glioma. *Eur J Nucl Med Mol Imaging* 2017;44(3):392–7.
  82. Bashir A, Brennum J, Broholm H, et al. The diagnostic accuracy of detecting malignant transformation of low-grade glioma using O-(2-[18F] fluoroethyl)-L-tyrosine positron emission tomography: a retrospective study. *J Neurosurg* 2018;130(2):451–64.
  83. Galldiks N, Stoffels G, Ruge MI, et al. Role of O-(2-18F-fluoroethyl)-L-tyrosine PET as a diagnostic tool for detection of malignant progression in patients with low-grade glioma. *J Nucl Med* 2013;54(12):2046–54.
  84. Lohmann P, Stavrinou P, Lipke K, et al. FET PET reveals considerable spatial differences in tumour burden compared to conventional MRI in newly diagnosed glioblastoma. *Eur J Nucl Med Mol Imaging* 2019;46(3):591–602.
  85. Song S, Cheng Y, Ma J, et al. Simultaneous FET-PET and contrast-enhanced MRI based on hybrid PET/MR improves delineation of tumor spatial biodistribution in gliomas: a biopsy validation study. *Eur J Nucl Med Mol Imaging* 2020;47(6):1458–67.
  86. Verburg N, Koopman T, Yaqub MM, et al. Improved detection of diffuse glioma infiltration with imaging combinations: a diagnostic accuracy study. *Neuro Oncol* 2020;22(3):412–22.

87. Hirata T, Kinoshita M, Tamari K, et al. <sup>11</sup>C-methionine-<sup>18</sup>F-FDG dual-PET-tracer-based target delineation of malignant glioma: evaluation of its geometrical and clinical features for planning radiation therapy. *J Neurosurg* 2019;131(3):676–86.
88. Poulsen SH, Urup T, Grunnet K, et al. The prognostic value of FET PET at radiotherapy planning in newly diagnosed glioblastoma. *Eur J Nucl Med Mol Imaging* 2017;44(3):373–81.
89. Kunz M, Albert NL, Unterrainer M, et al. Dynamic <sup>18</sup>F-FET PET is a powerful imaging biomarker in gadolinium-negative gliomas. *Neuro Oncol* 2019; 21(2):274–84.
90. Molinaro AM, Hervey-Jumper S, Morshed RA, et al. Association of maximal extent of resection of contrast-enhanced and non-contrast-enhanced tumor with survival within molecular subgroups of patients with newly diagnosed glioblastoma. *JAMA Oncol* 2020;6(4):495–503.
91. Suchorska B, Jansen NL, Linn J, et al. Biological tumor volume in <sup>18</sup>FET-PET before radiochemotherapy correlates with survival in GBM. *Neurology* 2015;84(7):710–9.
92. Bette S, Peschke P, Kaesmacher J, et al. Static FET-PET and MR imaging in anaplastic gliomas (WHO III). *World Neurosurg* 2016;91:524–531 e521.
93. Holzgreve A, Albert NL, Galldiks N, et al. Use of PET Imaging in neuro-oncological surgery. *Cancers (Basel)* 2021;13(9):2093.
94. Floeth FW, Sabel M, Ewelt C, et al. Comparison of (<sup>18</sup>)F-FET PET and 5-ALA fluorescence in cerebral gliomas. *Eur J Nucl Med Mol Imaging* 2011;38(4): 731–41.
95. Werner JM, Weller J, Ceccon G, et al. Diagnosis of pseudoprogression following temozolamide chemoradiation in newly diagnosed glioblastoma patients using FET-PET. *Clin Cancer Res* 2021;27(13):3704–13.
96. Galldiks N, Dunkl V, Stoffels G, et al. Diagnosis of pseudoprogression in patients with glioblastoma using O-(2-[<sup>18</sup>F]fluoroethyl)-L-tyrosine PET. *Eur J Nucl Med Mol Imaging* 2015;42(5):685–95.
97. Werner JM, Stoffels G, Lichtenstein T, et al. Differentiation of treatment-related changes from tumour progression: a direct comparison between dynamic FET PET and ADC values obtained from DWI MRI. *Eur J Nucl Med Mol Imaging* 2019; 46(9):1889–901.
98. Kebir S, Fimmers R, Galldiks N, et al. Late pseudoprogression in glioblastoma: diagnostic value of dynamic O-(2-[<sup>18</sup>F]fluoroethyl)-L-Tyrosine PET. *Clin Cancer Res* 2016;22(9):2190–6.
99. Bashir A, Mathilde Jacobsen S, Molby Henriksen O, et al. Recurrent glioblastoma versus late posttreatment changes: diagnostic accuracy of O-(2-[<sup>18</sup>F]fluoroethyl)-L-tyrosine positron emission tomography (18F-FET PET). *Neuro Oncol* 2019;21(12):1595–606.
100. Galldiks N, Stoffels G, Filss CP, et al. Role of O-(2-(<sup>18</sup>F)fluoroethyl)-L-tyrosine PET for differentiation of local recurrent brain metastasis from radiation necrosis. *J Nucl Med* 2012;53(9):1367–74.
101. Heiss WD, Wienhard K, Wagner R, et al. F-Dopa as an amino acid tracer to detect brain tumors. *J Nucl Med* 1996;37(7):1180–2.
102. Chen W, Silverman DH, Delaloye S, et al. <sup>18</sup>F-FDOPA PET imaging of brain tumors: comparison study with <sup>18</sup>F-FDG PET and evaluation of diagnostic accuracy. *J Nucl Med* 2006;47(6): 904–11.
103. Huang SC, Yu DC, Barrio JR, et al. Kinetics and modeling of L-6-[<sup>18</sup>F]fluoro-dopa in human positron emission tomographic studies. *J Cereb Blood Flow Metab* 1991;11(6):898–913.
104. Tatekawa H, Hagiwara A, Yao J, et al. Voxelwise and patientwise correlation of (<sup>18</sup>)F-FDOPA PET, relative cerebral blood volume, and apparent diffusion coefficient in treatment-naïve diffuse gliomas with different molecular subtypes. *J Nucl Med* 2021;62(3):319–25.
105. Jena A, Taneja S, Khan AA, et al. Recurrent glioma: does qualitative simultaneous <sup>18</sup>F-DOPA PET/mp-MRI improve diagnostic workup? An initial Experience. *Clin Nucl Med* 2021;46(9):703–9.
106. Shoup TM, Olson J, Hoffman JM, et al. Synthesis and evaluation of [<sup>18</sup>F]1-amino-3-fluorocyclobutane-1-carboxylic acid to image brain tumors. *J Nucl Med* 1999;40(2):331–8.
107. Michaud L, Beattie BJ, Akhurst T, et al. <sup>18</sup>F-Fluciclovine ((<sup>18</sup>)F-FACBC) PET imaging of recurrent brain tumors. *Eur J Nucl Med Mol Imaging* 2020; 47(6):1353–67.
108. Laudicella R, Quartuccio N, Argiroffi G, et al. Unconventional non-amino acidic PET radiotracers for molecular imaging in gliomas. *Eur J Nucl Med Mol Imaging* 2021;48(12):3925–39.
109. Ruan S, Zhou Y, Jiang X, et al. Rethinking CRITID Procedure of Brain targeting drug delivery: circulation, blood brain barrier recognition, intracellular transport, diseased cell targeting, internalization, and drug release. *Adv Sci (Weinh)* 2021;8(9): 2004025.
110. Pike VW. PET radiotracers: crossing the blood-brain barrier and surviving metabolism. *Trends Pharmacol Sci* 2009;30(8):431–40.
111. Rohrich M, Loktev A, Wefers AK, et al. IDH-wild-type glioblastomas and grade III/IV IDH-mutant gliomas show elevated tracer uptake in fibroblast activation protein-specific PET/CT. *Eur J Nucl Med Mol Imaging* 2019;46(12):2569–80.
112. Vettermann FJ, Harris S, Schmitt J, et al. Impact of TSPO receptor Polymorphism on [(<sup>18</sup>)F]GE-180 binding in healthy brain and Pseudo-reference

- regions of Neurooncological and Neurodegenerative Disorders. *Life (Basel)* 2021;11(6):484.
113. Salas Fragomeni RA, Menke JR, Holdhoff M, et al. Prostate-specific membrane antigen-targeted imaging with [<sup>18</sup>F]DCFPyL in high-grade gliomas. *Clin Nucl Med* 2017;42(10):e433–5.
114. Verma P, Malhotra G, Goel A, et al. Differential uptake of <sup>68</sup>Ga-PSMA-HBED-CC (PSMA-11) in low-grade versus high-grade gliomas in treatment-Naive patients. *Clin Nucl Med* 2019;44(5):e318–22.
115. Liu D, Cheng G, Ma X, et al. PET/CT using (<sup>68</sup>)Ga-PSMA-617 versus (<sup>18</sup>)F-fluorodeoxyglucose to differentiate low- and high-grade gliomas. *J Neuroimaging* 2021;31(4):733–42.
116. Holzgreve A, Biczok A, Ruf VC, et al. PSMA Expression in Glioblastoma as a basis for theranostic approaches: a retrospective, correlational panel study including immunohistochemistry, clinical parameters and PET Imaging. *Front Oncol* 2021;11: 646387.
117. Andrei Iagaru M, Camila Mosci M, Erik Mittra M, et al. Glioblastoma multiforme recurrence: an Exploratory study of <sup>18</sup>F FPPRGD2 PET/CT. *Radiology* 2015;277(2):497–506.
118. Santagata S, Ierano C, Trotta AM, et al. CXCR4 and CXCR7 signaling pathways: a focus on the cross-talk between cancer cells and tumor microenvironment. *Front Oncol* 2021;11:591386.
119. Shooli H, Nemati R, Ahmadzadehfar H, et al. Theranostics in brain tumors. *PET Clin* 2021;16(3): 397–418.
120. Huang X, Bai H, Zhou H, et al. Performance of <sup>18</sup>F-FET-PET versus <sup>18</sup>F-FDG-PET for the diagnosis and grading of brain tumors: inherent bias in meta-analysis not revealed by quality metrics. *Neuro Oncol* 2016;18(7):1028.
121. Furuse M, Nonoguchi N, Yamada K, et al. Radiological diagnosis of brain radiation necrosis after cranial irradiation for brain tumor: a systematic review. *Radiat Oncol* 2019;14(1):28.
122. Seidlitz A, Beuthien-Baumann B, Lock S, et al. Final results of the prospective biomarker trial PETra: [<sup>11</sup>C]-MET-Accumulation in Postoperative PET/MRI predicts outcome after radiochemotherapy in glioblastoma. *Clin Cancer Res* 2021;27(5): 1351–60.
123. Mittlmeier LM, Suchorska B, Ruf V, et al. (<sup>18</sup>)F-FET PET uptake characteristics of long-term IDH-wild-type diffuse glioma Survivors. *Cancers (Basel)* 2021;13(13).
124. Lundemann M, Munck Af, Rosenschold P, et al. Feasibility of multi-parametric PET and MRI for prediction of tumour recurrence in patients with glioblastoma. *Eur J Nucl Med Mol Imaging* 2019; 46(3):603–13.
125. Suchorska B, Giese A, Biczok A, et al. Identification of time-to-peak on dynamic <sup>18</sup>F-FET-PET as a prognostic marker specifically in IDH1/2 mutant diffuse astrocytoma. *Neuro Oncol* 2018;20(2): 279–88.
126. Galldiks N, Dunkl V, Ceccon G, et al. Early treatment response evaluation using FET PET compared to MRI in glioblastoma patients at first progression treated with bevacizumab plus temozolamide. *Eur J Nucl Med Mol Imaging* 2018;45(13): 2377–86.
127. Oen SK, Aasheim LB, Eikenes L, et al. Image quality and detectability in Siemens Biograph PET/MRI and PET/CT systems-a phantom study. *EJNMMI Phys* 2019;6(1):16.
128. Lohmann P, Galldiks N, Kocher M, et al. Radiomics in neuro-oncology: basics, workflow, and applications. *Methods* 2021;188:112–21.
129. Pirotte B, Goldman S, Massager N, et al. Combined use of <sup>18</sup>F-fluorodeoxyglucose and <sup>11</sup>C-methionine in 45 positron emission tomography-guided stereotactic brain biopsies. *J Neurosurg* 2004; 101(3):476–83.